Proceeding Paper

Effects of Cesium/Formamidinium Co-Additions to Perovskite Solar Cells †

Ren Nonomura [1], Takeo Oku [1,*], Iori Ono [1], Atsushi Suzuki [1], Masanobu Okita [2], Sakiko Fukunishi [2], Tomoharu Tachikawa [2] and Tomoya Hasegawa [2]

[1] Department of Materials Science, The University of Shiga Prefecture, 2500 Hassaka, Hikone 522-8533, Shiga, Japan; ov21rnonomura@ec.usp.ac.jp (R.N.); ov21ishimaji@ec.usp.ac.jp (I.O.); suzuki@mat.usp.ac.jp (A.S.)
[2] Osaka Gas Chemicals Co., Ltd., 5-11-61 Torishima, Konohana-ku, Osaka 554-0051, Japan; okita@ogc.co.jp (M.O.); fukunishi@ogc.co.jp (S.F.); t-tachikawa@ogc.co.jp (T.T.); hasegawa_tomoya@ogc.co.jp (T.H.)
* Correspondence: oku@mat.usp.ac.jp; Tel.: +81-749-28-8368

† Presented at the 3rd International Electronic Conference on Applied Sciences; Available online: https://asec2022.sciforum.net/.

Abstract: The stabilities and conversion efficiencies of the perovskite solar cells by incorporating cesium (Cs) or formamidinium (FA) at the CH_3NH_3 site were investigated. Additive effects on the photovoltaic properties and crystalline structures were investigated by current-voltage measurements, X-ray diffraction, and scanning electron microscopy. The simultaneous co-addition of Cs and FA to the $CH_3NH_3PbI_3$ perovskite crystal improved the photovoltaic properties, which would be due to the suppression of decomposition of the perovskite crystals and promotion of crystal growth.

Keywords: perovskite; crystal structure; Pb-free; double perovskite; dimensionality; halide; solar cell; low dimensional perovskite

Citation: Nonomura, R.; Oku, T.; Ono, I.; Suzuki, A.; Okita, M.; Fukunishi, S.; Tachikawa, T.; Hasegawa, T. Effects of Cesium/Formamidinium Co-Additions to Perovskite Solar Cells. *Eng. Proc.* **2022**, *4*, x. https://doi.org/10.3390/xxxxx

Academic Editor(s):

Published: 1 December 2022

1. Introduction

Recently developed $CH_3NH_3PbI_3$ ($MAPbI_3$) perovskite solar cells have several advantages, such as tunable band gaps, easy fabrication process, and high conversion efficiencies [1–5]. However, the $MAPbI_3$ is typically unstable in air because of the migration of CH_3NH_3 (MA). Therefore, the stability of the perovskite solar cells should be improved, and one method to improve the stability is elemental adding to the perovskite compounds [5–7].

As formamidinium ($CH(NH_2)_2$, FA) have larger ionic radii (2.53 Å) than MA (2.17 Å), which can be expected to improve the structural stability [5]. Several studies on FA addition have been carried out, and the photovoltaic properties and stability of the $MAPbI_3$ were improved [8–11]. FA addition is expected to extend the carrier lifetime and to reduce the carrier recombination in the perovskite layers. In addition to the FA addition, various alkali cations and organic molecules such as cesium (Cs) [12–14], rubidium (Rb) [15–18], potassium (K) [19–23], sodium (Na) [24–27], guanidinium ($C(NH_2)_3$, GA) [28–31], or ethyl ammonium ($CH_3CH_2NH_2$, EA) [32,33], were added to stabilize the $MAPbI_3$ perovskite crystals, and the photovoltaic properties were improved by these additions.

Another approach to improve the stability of perovskite solar cells is introducing polysilane materials into the perovskite devices [34–36]. The polysilanes are p-type semiconductors, which promote hole transfer [37], and polysilanes are more stable at elevated temperatures above 300 °C than ordinary organic materials, which is expected as a protective layer when deposited on perovskite compounds [38,39].

The purpose of the present work is to fabricate and characterize perovskite solar cells in which a small amount of FA and Cs were added to $MAPbI_3$, and annealed at high temperature of 190 °C in ambient air applying the DPPS layer on the perovskite layer. The annealing temperature is higher than 140 °C, which may lead the stabilization of the perovskite grains.

2. Experimental Procedures

A schematic illustration showing the fabrication processes used to fabricate photovoltaic cells is shown in Figure 1. All processes were performed in air [40,41] by using air-blow methos, and the detailed are described in the previous paper [42,43]. Standard $MAPbI_3$ precursors with molar concentrations of MAI and $PbCl_2$ of 2.4 and 0.8 M, respectively, were prepared, and FAI and CsI-added precursors were also prepared. To stabilize the perovskite structure, FA abd Cs were co-added to the crystals. The DPPS solutions were prepared from decaphenylcyclopentasilane (SI-30-15, Osaka Gas Chemical, Osaka, Japan) and chlorobenzene [38].

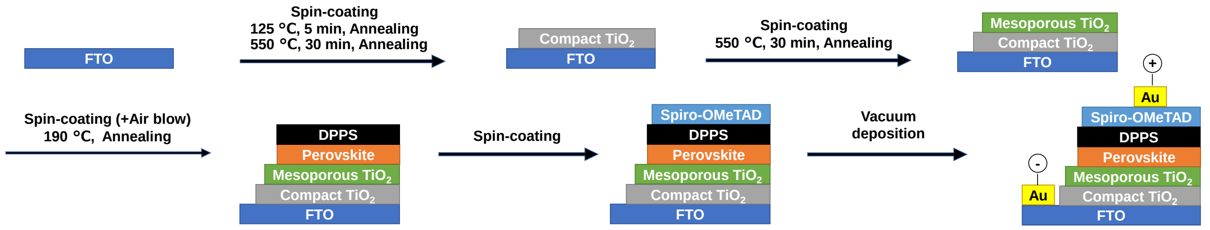

Figure 1. Schematic illustration for the fabrication process of the present photovoltaic cells.

3. Results and Discussion

The photovoltaic properties of the present perovskite solar cells were investigated using the *J*–*V* curves obtained under illumination, as shown in Figure 2a. The photovoltaic parameters, namely short-circuit current densities (J_{SC}), open-circuit voltages (V_{OC}), fill factor (FF), series resistance (R_s), shunt resistance (R_{sh}), photoconversion efficiency (η), averaged photoconversion efficiency (η_{ave}) and the energy gap (E_g) of all analyzed cells are listed in Table 2. The J_{SC} and η values increased by adding FA and Cs.

The EQE of the present devices including FAI and CsI are shown in Figure 2b. Energy gaps were calculated from the EQE spectra, and are listed in Table 2. The E_g values of Cs-added perovskites were higher than that of the standard $MAPbI_3$ crystal.

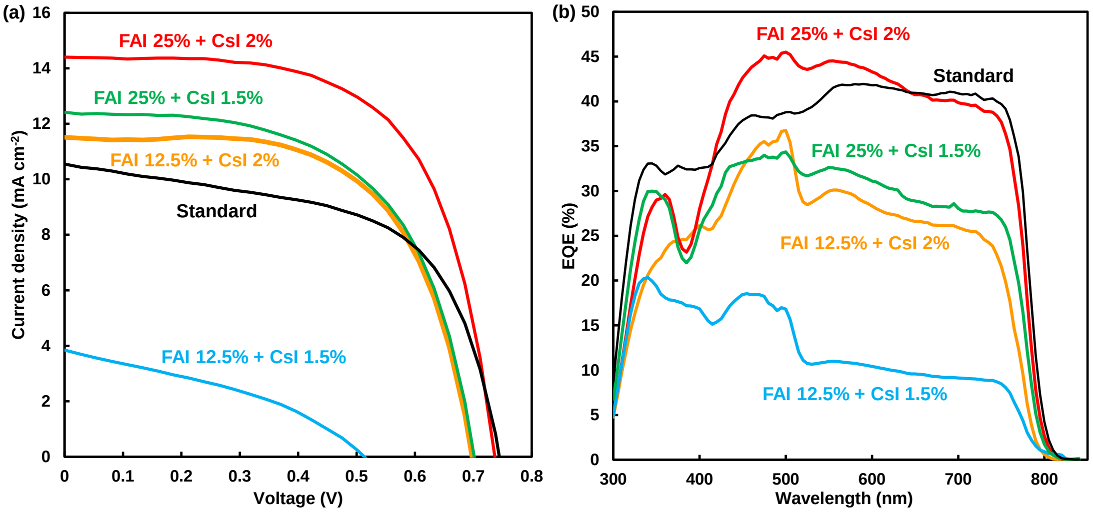

Figure 2. (**a**) *J-V* characteristics and (**b**) EQE of perovskite solar cells that contained FAI- and CsI-added perovskite.

Table 1. Measured photovoltaic parameters of the present perovskite solar cells.

Device		J_{SC}	V_{OC}	FF	R_S	R_{Sh}	η	η_{ave}	E_g
FAI (%)	**CsI (%)**	**(mA cm^{-2})**	**(V)**		**(Ω cm^2)**	**(Ω cm^2)**	**(%)**	**(%)**	**(eV)**
0	0	10.55	0.744	0.585	1.49	325	4.59	4.17	1.544
12.5	1.5	3.84	0.513	0.364	2.26	224	0.72	0.61	1.554
12.5	2	11.52	0.698	0.623	1.90	8200	5.00	4.30	1.563
25	1.5	12.41	0.701	0.587	1.68	2654	5.11	4.77	1.549
25	2	14.41	0.737	0.634	1.71	10,338	6.73	6.38	1.548

XRD patterns and lattice constants of the perovskite compound in the present devices are shown in Figure 3 and Table 2. An intensity of the 100 peak for the FAI 25% and CsI 3% added device increased, and the crystal orientation of the I_{100}/I_{210} ratio increased from 3.0 to 9.7, as listed in Table 2. This indicates crystal growth of (100)-oriented perovskite grains, and addition of a small amount of FA and Cs improved the crystal orientation and suppressed the grain boundaries in the perovskite layer. The crystal growth in the perovskite layer would reduce the trap density between perovskite grains and increase the J_{SC} and η.

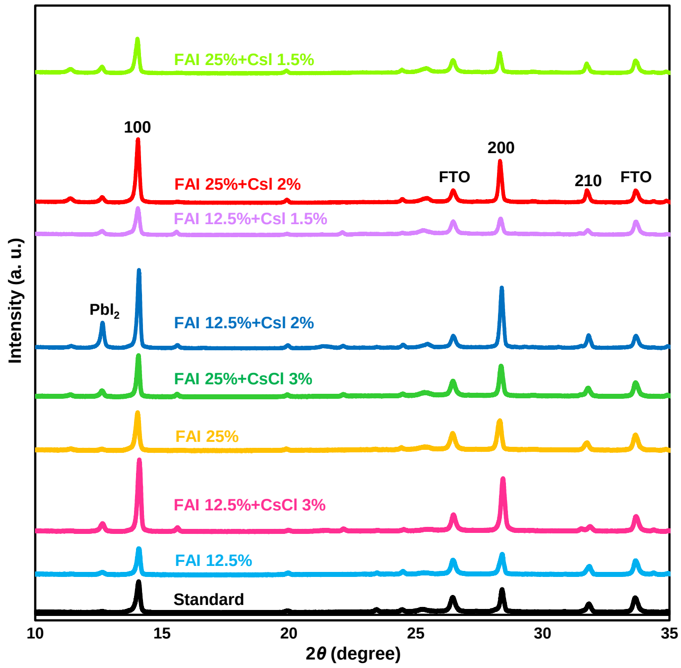

Figure 3. X-ray diffraction patterns of the present perovskite solar cells.

Table 2. Structural parameters of perovskite crystals with added FAI and CsCI.

Device			Lattice Constant (Å)	Crystallite Size (Å)	Orientation
FAI (%)	CsCI (%)	CsI (%)			I_{100}/I_{210}
0	0	0	6.279(2)	590	2.99
12.5	0	0	6.278(2)	671	2.62
12.5	3	0	6.272(2)	631	9.67
25	0	0	6.299(1)	579	3.84
25	3	0	6.286(1)	876	3.81
12.5	0	1.5	6.290(3)	545	4.46
12.5	0	2	6.282(0)	762	5.16
25	0	1.5	6.299(2)	592	3.05
25	0	2	6.297(1)	657	4.46

Elemental mappings arising from Cs K, Pb M, I L, Cl K, C K and N K lines are shown for the corresponding SEM images of the present perovskite solar cells, as shown in Figure 4. Perovskite particles with smaller sizes were distributed densely for the FAI and CsI-added devices, and each element was distributed homogeneously on the perovskite layer, and Cs atoms were also distributed in the perovskite layer. The elemental composition of Cl increased by the FA and Cs addition.

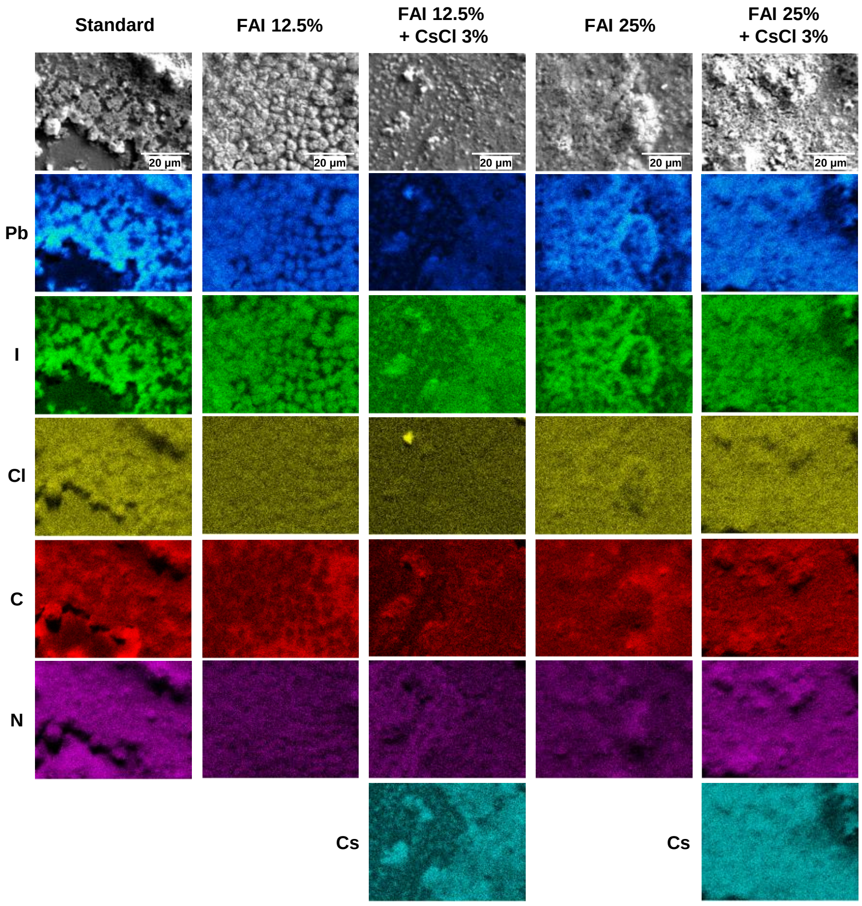

Figure 4. SEM images and corresponding elemental mappings of the present devices.

The changes in η of perovskite solar cells were investigated at 25 °C and 20% humidity for 42 days, as shown in Figure 5a. For the standard $MAPbI_3$ solar cell, the η decreased after 14 days. The degradation would be due to the decrease in photo-current by carrier recombination around defects which were formed by diffusion of MA cations and halogen anions for the long-term period. The η decrease was mitigated by the FA and Cs addition.

An energy level diagram of the cells is summarized as shown in Figure 5b. Previously reported values were also used for the energy levels. The electronic charge generation is caused by light irradiation from the FTO substrate side. The TiO_2 layer receives the electrons from the perovskite crystal, and the electrons are transported to the FTO. The holes are transported to an Au electrode through spiro-OMeTAD.

Table 3. Compositions of the solar cells as measured by EDS.

Device		Pb (at%)	I (at%)	Cl (at%)	C:N (at%)
FAI (%)	CsCl (%)				
0	0	30.3	57.0	12.7	38.6:61.4
12.5	0	29.7	57.7	12.7	48.3:51.7
12.5	3	39.4	32.1	28.4	33.7:66.3
25	0	30.0	59.1	10.9	44.8:55.2
25	3	27.4	63.0	9.57	36.6:63.4

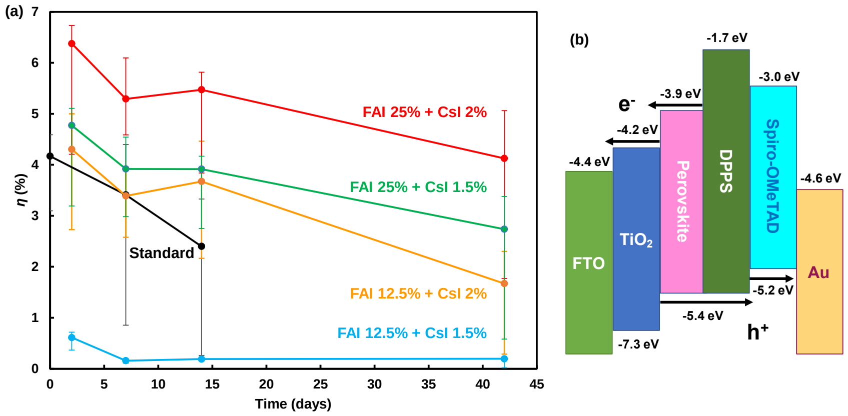

Figure 5. (**a**) Changes in efficiencies. (**b**) Energy level diagram.

4. Conclusions

The stabilities and conversion efficiencies of the perovskite solar cells were improved by incorporating Cs or FA at the CH_3NH_3 site. Additive effects on the photovoltaic properties and crystalline structures were investigated by *J-V* curve, XRD and SEM. The simultaneous co-addition of Cs and FA to the $CH_3NH_3PbI_3$ perovskite crystal improved the photovoltaic properties, which would be due to the suppression of decomposition of the perovskite crystals and the improvement of carrier transport.

Author Contributions: Conceptualization, R.N., T.O. and I.O.; Methodology, R.N., T.O., I.O. and A.S.; Formal Analysis, R.N., T.O., I.O. and A.S.; Investigation, R.N., T.O., I.O. and A.S.; Resources, M.O., S.F., T.T. and T.H.; Data Curation, R.N., T.O. and I.O.; Writing—Original Draft Preparation, R.N. and T.O.; Writing—Review & Editing, R.N., T.O., I.O., A.S., M.O., S.F., T.T. and T.H.; Project Administration, T.O.; Funding Acquisition, T.O. All authors have read and agreed to the published version of the manuscript.

Funding: This research was partly funded by Japan Society for the promotion of Science as a Grant-in-Aid for Scientific Research (C) 21K04809.

Institutional Review Board Statement: Not applicable.

Informed Consent Statement: Not applicable.

Data Availability Statement: Data is contained within the article.

Conflicts of Interest: The authors declare no conflict of interest.

References

1. Kojima, A.; Teshima, K.; Shirai, Y.; Miyasaka, T. Organometal halide perovskites as visible-light sensitizers for photovoltaic cells. *J. Am. Chem. Soc.* **2019**, *131*, 6050. https://doi.org/10.1021/ja809598r.
2. Kim, H.-S.; Lee, C.-R.; Im, J.-H.; Lee, K.-B.; Moehl, T.; Marchioro, A.; Moon, S.-J.; Humphry-Baker, R.; Yum, J.-H.; Moser, J.E.; et al. Lead iodide perovskite sensitized all-solid-state submicron thin film mesoscopic solar cell with efficiency exceeding 9%. *Sci. Rep.* **2012**, *2*, 591. https://doi.org/10.1038/srep00591.
3. Lee, M.M.; Teuscher, J.; Miyasaka, T.; Murakami, T.N.; Snaith, H.J. Efficient hybrid solar cells based on meso-superstructured organometal halide perovskites. *Science* **2012**, *338*, 643–647. https://doi.org/10.1126/science.1228604.
4. Burschka, J.; Pellet, N.; Moon, S.-J.; Humphry-Baker, R.; Gao, P.; Nazeeruddin, M.K.; Grätzel, M. Sequential deposition as a route to high-performance perovskite-sensitized solar cells. *Nature* **2013**, *499*, 316–320. https://doi.org/10.1038/nature12340.
5. Oku, T. Crystal structures of perovskite halide compounds used for solar cells. *Rev. Adv. Mater. Sci.* **2020**, *59*, 264–305. https://doi.org/10.1515/rams-2020-0015.
6. Saliba, M.; Orlandi, S.; Matsui, T.; Aghazada, S.; Cavazzini, M.; Correa-Baena, J.-P.; Gao, P.; Scopelliti, R.; Mosconi, E.; Dahmen, K.H.; et al. A molecularly engineered hole-transporting material for efficient perovskite solar cells. *Nat. Energy* **2016**, *1*, 15017. https://doi.org/10.1038/nenergy.2015.17.
7. Rao, M.K.; Sangeetha, D.N.; Selvakumar, M.; Sudhakar, Y.N.; Mahesha, M.G. Review on persistent challenges of perovskite solar cells' stability. *Sol. Energy* **2021**, *218*, 469–491. https://doi.org/10.1016/j.solener.2021.03.005.

8. Zhao, Y.; Tan, H.; Yuan, H.; Yang, Z.; Fan, J.Z.; Kim, J.; Voznyy, O.; Gong, X.; Quan, L.N.; Tan, C.S.; et al. Perovskite seeding growth of formamidinium-lead iodide-based perovskites for efficient and stable solar cells. *Nat. Commun.* **2018**, *9*, 1607. https://doi.org/10.1038/s41467-018-04029-7.
9. Suzuki, A.; Taguchi, M.; Oku, T.; Okita, M.; Minami, S.; Fukunishi, S.; Tachikawa, T. Additive effects of methyl ammonium bromide or formamidinium bromide in methylammonium lead iodide perovskite solar cells using decaphenylcyclopentasilane. *J. Mater. Sci. Mater. Electron.* **2021**, *32*, 26449–26464. https://doi.org/10.1007/s10854-021-07023-w.
10. Yang, W.S.; Park, B.W.; Jung, E.H.; Jeon, N.J.; Kim, Y.C.; Lee, D.U.; Shin, S.S.; Seo, J.; Kim, E.K.; Noh, J.H.; et al. Iodide management in formamidinium-lead-halide–based perovskite layers for efficient solar cells. *Science* **2017**, *356*, 1376–1379. https://doi.org/10.1126/science.aan2301.
11. Suzuki, A.; Kato, M.; Ueoka, N.; Oku, T. Additive effect of formamidinium chloride in methylammonium lead halide compound-based perovskite solar cells. *J. Electron. Mater.* **2019**, *48*, 3900–3907. https://doi.org/10.1007/s11664-019-07153-2.
12. Li, Z.; Yang, M.; Park, J.S.; Wei, S.H.; Berry, J.J.; Zhu, K. Perovskite structures by tuning tolerance factor: Formation of formamidinium and cesium lead iodide solid-state alloys. *Chem. Mater.* **2016**, *28*, 284–292. https://doi.org/10.1021/acs.chemmater.5b04107.
13. Yu, Y.; Wang, C.; Grice, C.R.; Shrestha, N.; Chen, J.; Zhao, D.; Liao, W.; Cimaroli, A.J.; Roland, P.J.; Ellingson, R.J.; et al. Improving the performance of formamidinium and cesium lead triiodide perovskite solar cells using lead thiocyanate additives. *ChemSusChem* **2016**, *9*, 3288–3297. https://doi.org/10.1002/cssc.201601027.
14. Ueoka, N.; Oku, T.; Suzuki, A.; Sakamoto, H.; Yamada, M.; Minami, S.; Miyauchi, S. Fabrication and characterization of $CH_3NH_3(Cs)Pb(Sn)I_3(Cl)$ perovskite solar cells with TiO_2 nanoparticle layers. *Jpn. J. Appl. Phys.* **2018**, *57*, 02CE03. https://doi.org/10.7567/JJAP.57.02CE03.
15. Zhang, M.; Yun, J.S.; Ma, Q.; Zheng, J.; Lau, C.F.J.; Deng, X.; Kim, J.; Kim, D.; Seidel, J.; Green, M.A.; et al. High-efficiency rubidium-incorporated perovskite solar cells by gas quenching. *ACS Energy Lett.* **2017**, *2*, 438−444. https://doi.org/10.1021/acsenergylett.6b00697.
16. Hu, Y.; Hutter, E.M.; Rieder, P.; Grill, I.; Hanisch, J.; Aygüler, M.F.; Hufnagel, A.G.; Handloser, M.; Bein, T.; Hartschuh, A.; et al. Understanding the role of cesium and rubidium additives in perovskite solar cells: Trap states, charge transport, and recombination *Adv. Energy Mater.* **2018**, *8*, 1703057. https://doi.org/10.1002/aenm.201703057.
17. Ueoka, N.; Oku, T.; Suzuki, A. Effects of doping with Na, K, Rb, and formamidinium cations on $(CH_3NH_3)_{0.99}Rb_{0.01}Pb_{0.99}Cu_{0.01}I_{3-x}(Cl, Br)_x$ perovskite photovoltaic cells. *AIP Adv.* **2020**, *10*, 125023. https://doi.org/10.1063/5.0029162.
18. Takada, K.; Oku, T.; Suzuki, A.; Okita, M.; Fukunishi, S.; Tachikawa, T.; Hasegawa, T. Fabrication and characterization of ethylammonium- and rubidium-added perovskite solar cells. *Chem. Proc.* **2022**, *9*, 14. https://doi.org/10.3390/IOCC_2022-12153.
19. Zheng, F.; Chen, W.; Bu, T.; Ghiggino, K.P.; Huang, F.; Cheng, Y.; Tapping, P.; Kee, T.W.; Jia, B.; Wen, X. Triggering the passivation effect of potassium doping in mixed-cation mixed-halide perovskite by light illumination. *Adv. Energy Mater.* **2019**, *9*, 1901016. https://doi.org/10.1002/aenm.201901016.
20. Kandori, S.; Oku, T.; Nishi, K.; Kishimoto, T.; Ueoka, N.; Suzuki, A. Fabrication and characterization of potassium- and formamidinium-added perovskite solar cells. *J. Ceram. Soc. Jpn.* **2020**, *128*, 805. https://doi.org/10.2109/jcersj2.20090.
21. Machiba, H.; Oku, T.; Kishimoto, T.; Ueoka, N.; Suzuki, A. Fabrication and evaluation of K-doped $MA_{0.8}FA_{0.1}K_{0.1}PbI_3(Cl)$ perovskite solar cells. *Chem. Phys. Lett.* **2019**, *730*, 117–123. https://doi.org/10.1016/j.cplett.2019.05.050.
22. Oku, T.; Kandori, S.; Taguchi, M.; Suzuki, A.; Okita, M.; Minami, S.; Fukunishi, S.; Tachikawa, T. Polysilane-inserted methylammonium lead iodide perovskite solar cells doped with formamidinium and potassium. *Energies* **2020**, *13*, 4776. https://doi.org/10.3390/en13184776.
23. Enomoto, A.; Suzuki, A.; Oku, T.; Okita, M.; Fukunishi, S.; Tachikawa, T.; Hasegawa, T. Effects of Cu, K and guanidinium addition to $CH_3NH_3PbI_3$ perovskite solar cells. *J. Electron. Mater.* **2022**, *51*, 4317–4328. https://doi.org/10.1007/s11664-022-09688-3.
24. Ueoka, N.; Oku, T. Effects of co-addition of sodium chloride and copper(ii) bromide to mixed-cation mixed-halide perovskite photovoltaic devices. *ACS Appl. Energy Mater.* **2020**, *9*, 24231. https://doi.org/10.1021/acsaem.0c00182.
25. Okumura, R.; Oku, T.; Suzuki, A.; Okita, M.; Fukunishi, S.; Tachikawa, T.; Hasegawa, T. Effects of adding alkali metals and organic cations to Cu-based perovskite solar cells. *Appl. Sci.* **2022**, *12*, 1710. https://doi.org/10.3390/app12031710.
26. Ueoka, N.; Oku, T.; Suzuki, A. Additive effects of alkali metals on Cu-modified $CH_3NH_3PbI_{3-\delta}Cl_\delta$ photovoltaic devices. *RSC Adv.* **2019**, *9*, 24231. https://doi.org/10.1039/c9ra03068a.
27. Suzuki, A.; Kitagawa, K.; Oku, T.; Okita, M.; Fukunishi, S.; Tachikawa, T. Additive effects of copper and alkali metal halides into methylammonium lead iodide perovskite solar cells. *Electron. Mater. Lett.* **2022**, *18*, 176–186. https://doi.org/10.1007/s13391-021-00325-5.
28. Tosado, G.A.; Zheng, E.; Yu, Q. Tuning cesium–guanidinium in formamidinium tin triiodide perovskites with an ethylenediammonium additive for efficient and stable lead-free perovskite solar cells. *Mater. Adv.* **2020**, *1*, 3507–3517. https://doi.org/10.1039/d0ma00520g.
29. Kishimoto, T.; Suzuki, A.; Ueoka, N.; Oku, T. Effects of guanidinium addition to $CH_3NH_3PbI_{3-x}Cl_x$ perovskite photovoltaic devices. *J. Ceram. Soc. Jpn.* **2019**, *127*, 491−497. https://doi.org/10.2109/jcersj2.18214.
30. Kishimoto, T.; Oku, T.; Suzuki, A.; Ueoka, N. Additive effects of guanidinium iodide on $CH_3NH_3PbI_3$ perovskite solar cells. *Phys. Status Solidi A* **2021**, *218*, 2100396. https://doi.org/10.1002/pssa.202100396.

31. Ono, I.; Oku, T.; Suzuki, A.; Asakawa, Y.; Terada, S.; Okita, M.; Fukunishi, S.; Tachikawa, T. Fabrication and characterization of $CH_3NH_3PbI_3$ solar cells with added guanidinium and inserted with decaphenylpentasilane. *Jpn. J. Appl. Phys.* **2022**, *61*, SB1024. https://doi.org/10.35848/1347-4065/ac2661.
32. Nishi, K.; Oku, T.; Kishimoto, T.; Ueoka, N.; Suzuki, A. Photovoltaic characteristics of $CH_3NH_3PbI_3$ perovskite solar cells added with ethylammonium bromide and formamidinium iodide. *Coatings* **2020**, *10*, 410. https://doi.org/10.3390/coatings10040410.
33. Terada, S.; Oku, T.; Suzuki, A.; Okita, M.; Fukunishi, S.; Tachikawa, T.; Hasegawa, T. Ethylammonium bromide- and potassium-added $CH_3NH_3PbI_3$ perovskite solar cells. *Photonics* **2022**, *9*, 791. https://doi.org/10.3390/photonics9110791.
34. Taguchi, M.; Suzuki, A.; Oku, T.; Fukunishi, S.; Minami, S.; Okita, M. Effects of decaphenylcyclopentasilane addition on photovoltaic properties of perovskite solar cells. *Coatings* **2018**, *8*, 461. https://doi.org/10.3390/coatings8120461.
35. Oku, T.; Nomura, J.; Suzuki, A.; Tanaka, H.; Fukunishi, S.; Minami, S.; Tsukada, S. Fabrication and characterization of $CH_3NH_3PbI_3$ perovskite solar cells added with polysilanes. *Int. J. Photoenergy* **2018**, *2018*, 8654963. https://doi.org/10.1155/2018/8654963.
36. Taguchi, M.; Suzuki, A.; Oku, T.; Ueoka, N.; Minami, S.; Okita, M. Effects of annealing temperature on decaphenylcyclopentasilane-inserted $CH_3NH_3PbI_3$ perovskite solar cells. *Chem. Phys. Lett.* **2019**, *737*, 136822. https://doi.org/10.1016/j.cplett.2019.136822.
37. Oku, T.; Nakagawa, J.; Iwase, M.; Kawashima, A.; Yoshida, K.; Suzuki, A.; Akiyama, T.; Tokumitsu, K.; Yamada, M.; Nakamura, M. Microstructures and photovoltaic properties of polysilane-based solar cells. *Jpn. J. Appl. Phys.* **2013**, *52*, 04CR07. https://doi.org/10.7567/JJAP.52.04CR07.
38. Oku, T.; Taguchi, M.; Suzuki, A.; Kitagawa, K.; Asakawa, Y.; Yoshida, S.; Okita, M.; Minami, S.; Fukunishi, S.; Tachikawa, T. Effects of polysilane addition to chlorobenzene and high temperature annealing on $CH_3NH_3PbI_3$ perovskite photovoltaic devices. *Coatings* **2021**, *11*, 665. https://doi.org/10.3390/coatings11060665.
39. Mizuno, S.; Oku, T.; Suzuki, A.; Okita, M.; Fukunishi, S.; Tachikawa, T.; Hasegawa, T. Photovoltaic properties and microstructures of polysilane-added perovskite solar cells. *Chem. Proc*. **2022**, *9*, 20. https://doi.org/10.3390/IOCC_2022-12169.
40. Oku, T.; Zushi, M.; Imanishi, Y.; Suzuki, A.; Suzuki, K. Microstructures and photovoltaic properties of perovskite-type $CH_3NH_3PbI_3$ compounds. *Appl. Phys. Express* **2014**, *7*, 121601. https://doi.org/10.7567/APEX.7.121601.
41. Ueoka, N.; Oku, T. Stability Characterization of PbI_2-added $CH_3NH_3PbI_{3-x}Cl_x$ photovoltaic devices. *ACS Appl. Mater. Interfaces* **2018**, *10*, 44443–44451. https://doi.org/10.1021/acsami.8b16029.
42. Oku, T.; Ohishi, Y.; Ueoka, N. Highly (100)-oriented $CH_3NH_3PbI_3$(Cl) perovskite solar cells prepared with NH_4Cl using an air blow method. *RSC Adv.* **2018**, *8*, 10389–10395. https://doi.org/10.1039/c7ra13582c.
43. Oku, T.; Ohishi, Y. Effects of annealing on $CH_3NH_3PbI_3$ (Cl) perovskite photovoltaic devices. *J. Ceram. Soc. Jpn.* **2018**, *126*, 56–60. https://doi.org/10.2109/jcersj2.17162.